TISSUE ENGINEERING
Volume 12, Number 5, 2006
© Mary Ann Liebert, Inc.

Direct Freeform Fabrication of Seeded Hydrogels in Arbitrary Geometries

DANIEL L. COHEN, Ph.D.,[1] EVAN MALONE, Ph.D.,[1] HOD LIPSON, Ph.D.,[1,2] and LAWRENCE J. BONASSAR, Ph.D.[1,3]

ABSTRACT

A major challenge in tissue engineering is the generation of cell-seeded implants with structures that mimic native tissue, both in anatomic geometries and intratissue cell distributions. By combining the strengths of injection molding tissue engineering with those of solid freeform fabrication (SFF), three-dimensional (3-D) pre-seeded implants were fabricated without custom-tooling, enabling efficient production of patient-specific implants. The incorporation of SFF technology also enabled the fabrication of geometrically complex, multiple-material implants with spatially heterogeneous properties that would otherwise be challenging to produce. Utilizing a custom-built robotic SFF platform and gel deposition tools, alginate hydrogel was used with calcium sulfate as a crosslinking agent to produce pre-seeded living implants of arbitrary geometries. The process was determined to be sterile and viable at 94 ± 5%. The GAG and hydroxyproline production was found to be similar to that of other implants fabricated using the same materials with different shaping methods. The geometric fidelity of the process was quantified by using the printing platform as a computerized measurement machine (CMM); the RMS surface roughness of printed samples in the z-dimension was found to be 0.16 ± 0.02 mm.

INTRODUCTION

THE GENERATION OF CELL-SEEDED IMPLANTS with structures that mimic native tissue, both in anatomic geometries and intratissue cell distributions, is a major challenge in tissue engineering. Indeed, the therapeutic promise of tissue engineering was most famously demonstrated in pioneering work by Charles Vacanti and colleagues in which tissue-engineered cartilage was shaped into the form of a human ear.[1] In additional work, this idea was extended to demonstrate the generation of cartilage of arbitrary shapes,[2] as well as many specific anatomic geometries including temporomandibular disc[3] and joint,[4] meniscus,[5] trachea,[6] intervertebral disc,[7] nasal tip,[8] and nasal septum.[9] These principles apply to other tissues as well, particularly bone, where the reproduction of anatomically shaped tissue has been demonstrated in the generation of femoral shaft[10] and mandibular condyle[4] in rats and culminating in the generation of a distal phalanx in a human patient.[11]

Previous studies demonstrating the engineering of tissues in complex geometries used a variety of techniques to achieve control of shape. Tissues with complex two-dimensional surface geometries have been generated by casting cell-seeded hydrogel onto substrate base layers with desired surface shapes.[12] Three-dimensional (3-D) tissues with complex geometries have been fabricated through seeding of cells onto molded scaffolds[13] or injection molding of cell-seeded hydrogels.[14] While these techniques were able to create constructs with complex shapes, they lacked the ability to easily create parts with spatial heterogeneities.

Other studies have investigated methods to reproduce zonal spatial variations in articular cartilage constructs.

[1]Department of Mechanical and Aerospace Engineering, [2]Department of Computer and Information Science, [3]Department of Biomedical Engineering, Cornell University, Ithaca, New York.

These approaches created spatially heterogeneous constructs by depositing multiple layers of chondrocytes[15] or chondrocyte-seeded hydrogels.[16,17] While these techniques produced zonal organization in engineered tissues, they were limited to spatially varying the construct properties along a single axis only. Furthermore, while these techniques were feasible in the case of *in vitro* construct fabrication, it is not inherently feasible to adapt them for *in vivo*, or *in situ*, fabrication. For example, it would be challenging to place pre-formed hydrogel sheets through a small orifice while achieving proper alignment and bonding, such as would be necessary for incorporation into a minimally invasive implantation scheme.

Solid freeform fabrication (SFF) technology has been used both to aid in the fabrication of tissues with complex geometries, as well to enable the production of constructs with spatial variations along multiple axes. SFF, often referred to as rapid prototyping, is analogous to 3-D printing. In SFF, layers of material are deposited or fused subsequently until a complete freeform geometry has been built.

SFF schemes have been used to engineer tissues with complex geometries by using rapid prototyping techniques and computer-aided manufacturing (CAM) to fabricate traditional porous scaffolds that are subsequently seeded with cells.[18] This approach was capable of creating scaffolds of high geometric complexity; however, problems inherent with traditional scaffolding techniques persisted, such as seeding-depth limitations. A second SFF-assisted approach to creating geometrically complex implants overcame seeding-depth limitations by rapid prototyping molds and injection of pre-seeded hydrogel.[19] A third SFF-based technique created pre-seeded geometrically complex implants without the need for a mold by photo-crosslinking PEO and PEGM layer-by-layer.[20] However, none of these three SFF-based techniques enabled the fabrication of implants with complex zonal variations in three dimensions (i.e., 3-D spatial variation in cell-type, cell density, etc.). Furthermore, these techniques are not ideal for minimally invasive implantation schemes. The SFF of traditional porous scaffolds[18] and molds[19] relied on *in vitro* fabrication of the implants and likely require invasive surgery to implant a full-sized construct. The photo-crosslinking technique[20] is not completely suitable for *in situ* fabrication because it imposes major constraints upon the environment in which constructs may be fabricated. For example, in the case of *in vivo* fabrication, it may not be feasible to separate the tissue of the patient widely and steadily enough for a pool of polymer to be maintained in a stable fashion. Also, it may be difficult to fit a light source into the fabrication cavity at an orientation that is nearly perpendicular to the direction of the filling of the polymer well. Additionally, orientation of the layers is important with SFF, due to the orientation's impact on mechanical properties; however, the photo-crosslinking technique is restricted to creating layer orientation in a direction perpendicular to gravity because the orientation of the surface of the liquid polymer pool is governed by gravitational force. The disadvantageous constraints imposed upon the printing environment by the polymer pool are also shared by techniques that deposit hydrogel into baths of crosslinkers.[21]

More recently, studies have investigated approaches using SFF technology that were capable of producing cell constructs with both geometric complexity and multi-axial zonal organization. Collagen I and pluronic F-127 were recently used in an SFF process to produce viable cell-gel constructs with complex geometries layer-by-layer.[22] While the technology was also capable of fabricating components with complex zonal organization,[22] constructs created with PF-127 and collagen I are generally not three dimensionally stable in culture. Furthermore, since the gelation was not initiated prior to the deposition of the material, but rather by means of heat flow, strict thermal constraints were placed upon the fabrication environment, which may adversely affect certain *in situ* or *in vivo* fabrication approaches. Thus, no SFF processes exist to create pre-seeded, arbitrarily shaped, spatially heterogeneous constructs that are three dimensionally stable in culture and minimally impose constraints upon the printing environment.

The approach presented herein used a gantry robot to deposit pre-seeded alginate hydrogel layer-by-layer. This technology was capable of producing implants with both complex geometry and zonal organization that were three dimensionally stable in culture. Since the gel was pre-seeded and crosslinking was initiated prior to deposition, this technique relaxed the constraints imposed upon the printing environment because, unlike other techniques, it neither required seeding of the construct after deposition nor required added energy to the material during deposition, such as specific light or temperature conditions. The only energy needed during deposition was that required to extrude the gel; this power source can easily be located externally to the printing environment without interfering with the *in situ* printing objective, unlike light and thermal energy sources. Alginate serves as a favorable cell delivery material since it is: 1) three dimensionally stable in culture, 2) non-toxic, 3) extrusion compatible, 4) pre-seeding compatible, and 5) crosslinking can be initiated prior to deposition.

The objectives of this study were to: 1) develop a process to print pre-cell-seeded alginate gels in arbitrary shapes; 2) document the sterility and viability of the process; 3) determine the mechanical properties and extracellular matrix production characteristics of printed samples; and 4) characterize the geometric fidelity of the printing technique.

MATERIALS AND METHODS

Robotic platform

The solid freeform fabrication robotic platform was an open-architecture CAM system that consisted of a gantry robot and a set of interchangeable deposition tools (Fig. 1).[23] The deposition tools were attached to the X-Y axes of the gantry robot, and the hydrogel was deposited onto the Z stage, which served as the build surface.

The gantry robot had a workspace of 30 × 30 × 30 cm and was capable of carrying a deposition tool of up to 5 kg. The X-Y axes of the gantry had a maximum traverse speed of 0.05 m/s and a maximum acceleration of 2.1 *g*. High traverse acceleration was important in order to maintain constant velocity around corners with small radii of curvature. The gantry robot could position the tip of the deposition tool with 25 μm precision.

The deposition tool was a linear actuator-driven syringe with interchangeable syringe tips that served as nozzles of various diameters, ranging from 0.33 to 0.84 mm. The maximum volumetric flow rate was 1.4 mL/s. A disposable syringe served as the material bay of the deposition tool. The material bay simply slid out of the deposition tool to facilitate multiple-material print jobs in which the material cartridge was frequently interchanged in mid-print.

Once the system was loaded with printing material, a CAD model was sent to the robot's control system in stereolithography (STL) format, a computer file format commonly used in rapid prototyping applications. Custom-written software sliced the model and planned tool paths within each layer. The tool-path planner prescribed a contour boundary path followed by raster fill-paths. The trajectory was sent from the computer to the robot and printing commenced (Fig. 2).

Cell isolation and culture

Cartilage was harvested from the femeropatellar groove of 1- to 3-day-old calves. The tissue was digested for 18 h at 37°C and 5% CO_2 in Dulbecco's modified Eagle medium (DMEM) containing 0.3% collagenase. The digest solution was filtered with a 100 μm cell strainer. The articular chondrocytes were isolated from the strained digest solution by centrifugation at 412 *g* for 7 min. Cells were washed twice with phosphate-buffered saline (PBS).[24] The initial viability was determined using trypan blue (Mediatech, Herndon, VA).

Samples were cultured in DMEM with 10% fetal bovine serum. A 1% antibiotic-antimyotic (10,000 U/mL penicillin G sodium, 10,000 μg/mL streptomycin sulfate, 25 μg/mL amophoterocin B in 0.85% saline) was also added to the growth medium, except during the sterility test. The cells were cultured at 37°C and 5% CO_2.[14]

Gel deposition

During the printing experiments, a tip diameter of 0.84 mm was selected. The robot planned the tool paths

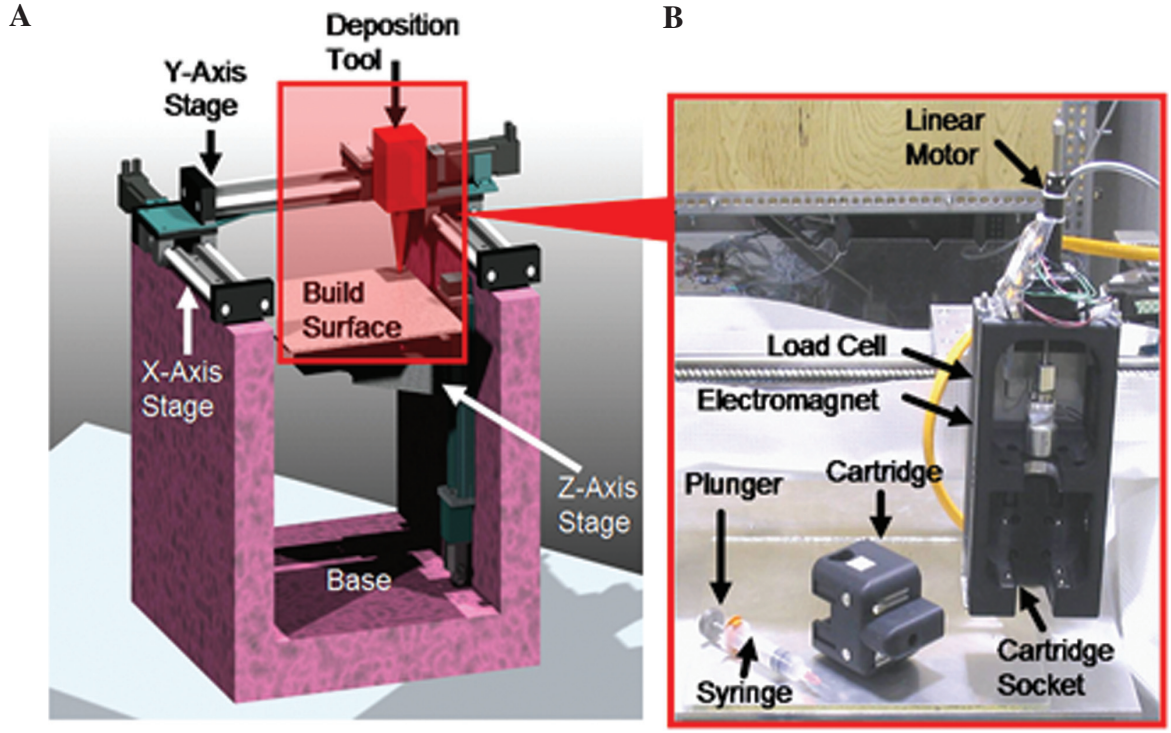


FIG. 1. Robotic printing platform. (**A**) CAD rendering of gantry robot. (**B**) Close-up view of deposition tool. (Color images are available online at www.liebertonline.com/ten).

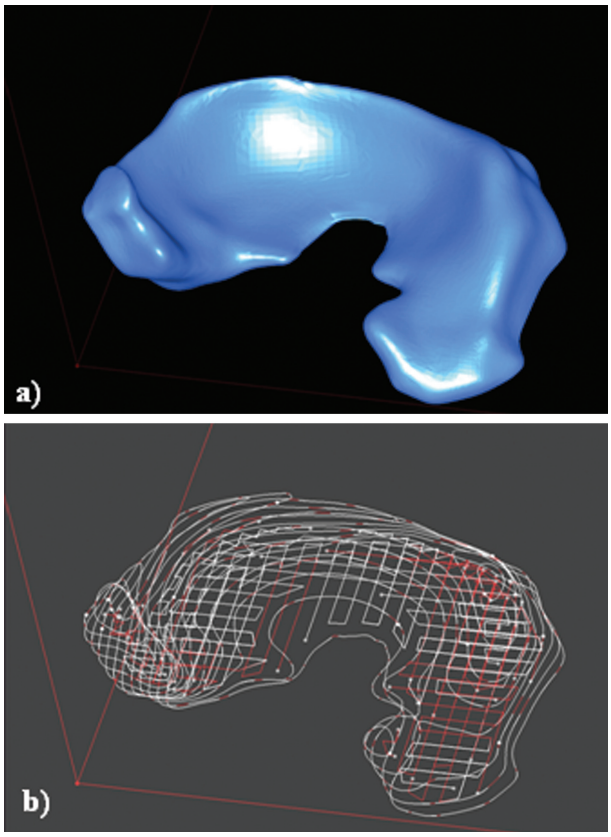


FIG. 2. Screenshot of trajectory planner. (**a**) CAD model loaded into trajectory planning software before tool-path generation. (**b**) Planned tool-paths. (Color images are available online at www.liebertonline.com/ten).

for material streams with a width of 1.2 mm and a height of 0.8 mm. The gel flow rate was 0.6 mL/min. At the start of each new path, the deposition started 0.2 s before the motion of the gantry robot.

Chemical formulation and cell encapsulation

The chondrocytes were suspended in PBS and spun-down into a pellet with a centrifuge. Low-viscosity, high G-content non-medical grade LF10/60 alginate (FMC Biopolymer, Drammen, Norway) was dissolved at a concentration of 20 mg/mL, passed through a 0.22 μm filter, and added to the cell pellet to achieve a density of 50×10^6 cells/mL. The alginate-cell suspension was vortexed and mixed in a 2:1 ratio with autoclaved 10 mg/mL $CaSO_4$ in PBS. After mixing, the resulting hydrogel had a cell density of 33×10^6 cells/mL. Due to the time-dependent gelation process, the window for optimal printing was ~15 min from the time that the crosslinker is mixed with the alginate. The hydrogel was loaded into a syringe and inserted into the deposition tool.

Viability test

The viability of the deposition process was measured by testing viability immediately before and after the printing process. The process viability was defined as the ratio of cell viability after harvesting but before gel seeding to the cell viability immediately after deposition. Twenty-four disks, 6 mm in diameter $\times$ 2 mm in height, were printed into a 24-well plate. Each sample was pulled from the plate and tested with the Live/Dead Viability Assay (Molecular Probes, Eugene, OR). The samples were exposed to 0.15 μM calcein AM and 2 μM ethidium homodimer-1 (EthD-1) for 60 min at room temperature. The stained samples were analyzed under a Nikon TE2000-S microscope equipped with an epiflourescence attachment and a Spot RT digital camera. The viability was calculated as the average of the ratios of live over total cells in a given field.

Sterility

An empty autoclave bag was sealed and autoclaved. The sealed bag was placed under a sterile hood, a slit was cut into the bottom end of the bag, and a sterile 24-well plate was inserted. The bag was resealed with tape and ready for printing. The autoclave bag served as a sterile envelope around the plate, which protected the printed samples from contamination.

To test the effectiveness of the envelope concept, 24 disks, 6 mm in diameter $\times$ 2 mm in height, were printed into an envelope-protected sterile plate and cultured for 8 days without antibiotics or antimyotics. After the incubation period, media from each well were pulled and tested for bacterial presence with 100 μM BacLight Green Stain (Molecular Probes), according to the manufacturer's instructions. Bacterial counts were performed using a hemacytometer (Hausser Scientific, Horsham, PA) and a Nikon TE2000-S microscope equipped with an epiflourescence attachment and a digital camera.

DNA content and ECM accumulation

Disks, 6 mm $\times$ 2 mm, were printed into a 24-well plate. The disks were cultured for a period of time ranging from 0 to 142 days. Disks were removed from culture, weighed, lyophilized, and weighed again. All of the dry samples were digested in 1 mL of papain digest buffer (0.1 mol/L sodium phosphate, 10 mmol sodium EDTA [BDH], 10 mmol cysteine hydrochloride [Sigma-Aldrich, St. Louis, MO], and 3.8 U/mL papain [Sigma]) at 65°C for 24 h.

The digest was analyzed for DNA content, as a marker of cell quantity. The assay was carried out in 96-well plates (Nalge Nunc, Rochester, NY). In each well, 190 μL of 0.1 μg/mL Hoechst 33258 dye in TES buffer was added to 10 μL of the digested samples. Calf thymus DNA was used as a standard and the absorbance was read

using a Tecan microplate reader with the excitation wavelength set at 348 nm and the emission wavelength set at 456 nm.[25]

The digest was also analyzed for glycosaminoglycans (GAG) as a marker of proteoglycans. The assay was carried out in 96-well plates. In each well, 50 μL of digest was mixed with 250 μL of dye containing 16 mg/L 1,9-dimethylmethylene blue (DMMB) and 3.04 g/L glycine (pH 1.5). The absorbance was read at 595 nm using a microplate reader. Chondroitin-6-sulfate from shark cartilage (Sigma) was used to construct the standard curve.[26]

Additionally, the digest was analyzed for hydroxyproline as a marker of collagen. One hundred μL of each sample's digest was hydrolyzed in 100 μL of 2N NaOH at 110°C for 18 h. The following were combined into screw-cap microfuge tubes: 20 μL 5N HCl, 100 μL digested hydrolyzed sample, 100 μL 0.01 M $CuSO_4$, 100 μL 2.5 N NaOH, and 100 μL 6% H_2O_2. After the addition of H_2O_2, the tubes were allowed to sit at room temperature for about 5 min while being shaken occasionally to remove gas bubbles. The tubes were then vortexed and placed in a heat block at 80°C for 5 min. The tubes were placed in an ice bath until cooled to room temperature. Four hundred μL of 3N H_2SO_4 and 200 μL of DMAB were added to each tube. Each well of a 96-well plate was filled with 200 μL of a treated sample and absorbance was read at 540 nm.[27]

Mechanical characterization

Disks less than 1-hour-old, 6 mm $\times$ 2 mm, were printed and placed in an ELF 3200 (EnduraTec, Minnetonka, MN) mechanical test-frame in an unconfined compression chamber between two parallel plates. A 1000 g load cell (Sensotec, Columbus, OH) was attached to the bottom plate and a displacement sensor to the top plate. The bottom plate was filled with PBS in order to completely encompass the sample with fluid. The two plates started at a distance corresponding to 0% strain and stepped 0.1 mm towards each other every 100 s until 45% strain was achieved. Stress and strain data were acquired at a frequency of 5 Hz.[28]

The stress-strain curve of each printed sample was analyzed by first finding the equilibrium stress corresponding to each imposed strain (0–45%). The linear region of the equilibrium stress-strain curve was fit linearly; the slope of this line was the Young's modulus of the sample.

Geometric fidelity

The geometric fidelity of the printing process was determined by using the printing platform as a coordinate measuring machine (CMM). A metal needle was attached to the deposition tool with a wire soldered to the needle. Another wire was attached to the metal base plate of the printer and an electrical power source. Since the hydrogels being measured were electrically conductive, when the needle touched the alginate hydrogel, current flowed from the power source through the base plate, through the hydrogel sample, and back to the tip–thus completing the electrical circuit. Positional data was logged when the robot sensed that the electrical circuit was completed. By stepping over the entire part in 0.35 mm X-Y coordinate increments, a map of the surface points of the hydrogel sample was constructed.

Using the surface map, the average height of the X-Y plane boundary points was calculated, these points representing the height of the base plate. The Z coordinates of all points were shifted down by the mean boundary height in order to align the base plate with the X-Y plane. The list of points was truncated to exclude all points that represented the base plate itself (i.e., all points with zero-valued Z coordinates were removed). The mean X and Y coordinates were calculated and then the X and Y coordinates of the points were shifted by the mean values in order to center the samples in the X-Y plane.

The overall average height of the sample was calculated by finding the mean z-value of the points. The average height, excluding the edge effect, was calculated by finding the mean z-value of the points that were in the inner X-Y region of the geometry; that is, all points whose X and Y coordinates fell within 90 $\times$ 90% of the total X-Y cross-section. The RMS surface roughness was determined to be the standard deviation of these inner points.

In order to calculate the X-Y geometric fidelity, the point list was further truncated to exclude all points with z-values below half the total average height; doing so removes the effect of the sloping interface between the walls of the geometry and the base plate. The X-Y boundary points were identified using a standard convex hull

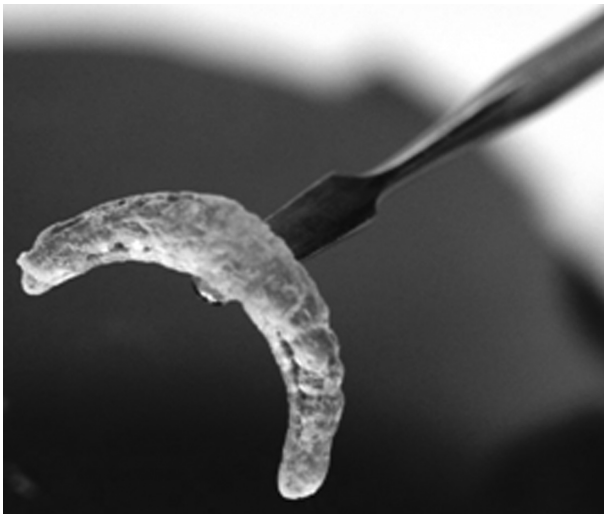


FIG. 3. Printed crescent suspended with tool.

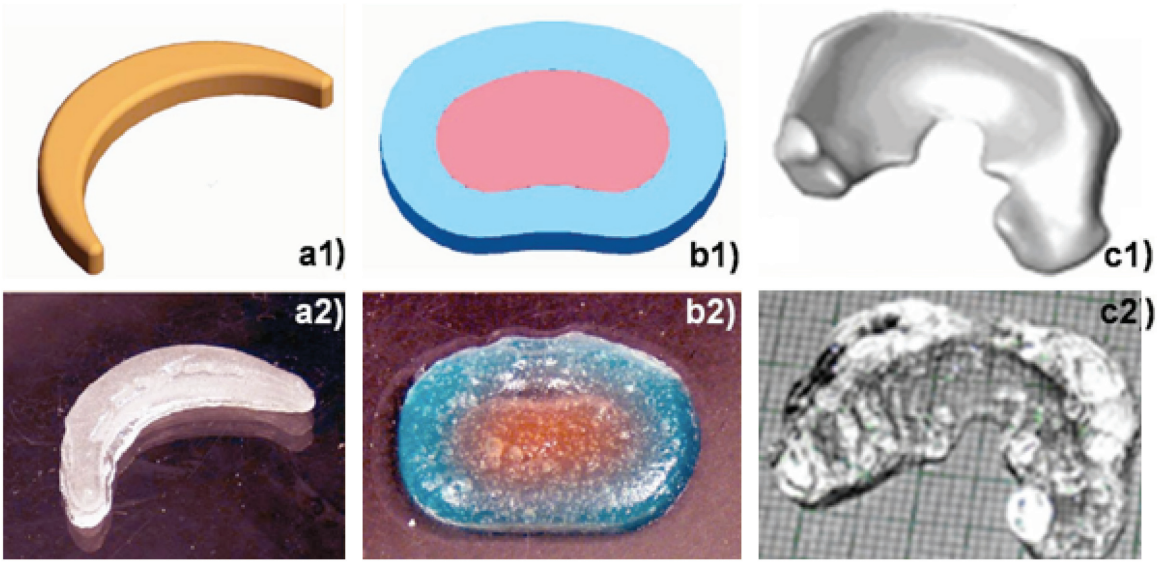


FIG. 4. CAD models and photographs of printed samples. (Color images are available online at www.liebertonline.com/ten).

algorithm, "convhull," in Matlab (MathWorks, Natick, MA). These X-Y boundary points were subtracted by the intended X-Y coordinate corresponding to each point in order to generate an X-Y error map. The mean and standard deviation of this error were calculated to reflect the X-Y geometric fidelity.

RESULTS

Spatially heterogeneous gel constructs

A set of gel constructs was created to showcase the ability of the system to fabricate complex, spatially heterogeneous hydrogel geometries. A crescent-shaped part, 2.5 cm long × 0.75 cm wide, was printed and elevated with a thin utensil to verify that the part maintained its shape while fully supporting its weight (Fig. 3). The crescent-shaped part was drawn in the SolidWorks CAD program (Fig. 4a1), input into the printer's control software, and printed (Fig. 4a2).

To verify the system's ability to construct a multiple-material, spatially heterogeneous construct, an IV disc-shaped CAD model was generated (Fig. 4b1), processed with the robot's control software, and printed (Fig. 4b2). The two-material component was fabricated from two different batches of alginate hydrogel, each stained with

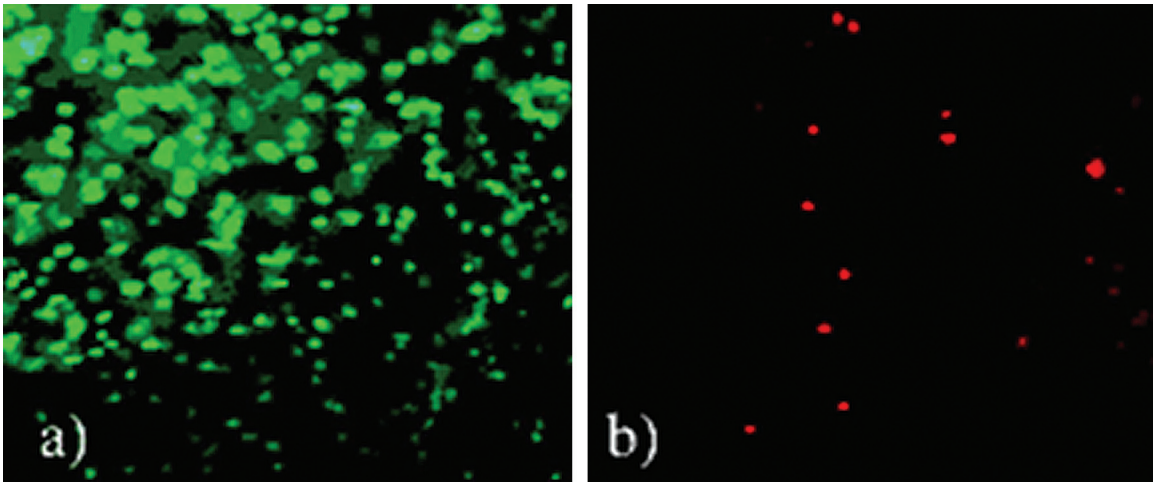


FIG. 5. Live and dead panels of the same view field from the viability test. (Color images are available online at www.liebert online.com/ten).

a dye of a different color. Utilizing the multiple-material capabilities of the robotic platform, the robot stopped at numerous points throughout the print and requested a change of materials, as prescribed by the robot's tool path planner. At each of these points, the material bay and syringe tip unit of the deposition tool were manually swapped with the designated material bay/syringe tip unit and printing commenced.

In order to demonstrate the system's ability to create implants with complex geometries, a CAD model of an ovine meniscus was constructed from a CT scan (Fig. 4c1) and printed (Fig. 4c2).

Viability and sterility

Viability tests successfully detected both live (Fig. 5a) and dead (Fig. 5b) cells in printed gels. The viability of the printing process was determined to be 94 ± 5% (n = 15). The viability appeared to be spatially uniform. By inspection with phase contrast microscopy and fluorescence microscopy, the cell distribution was observed to be homogeneous. When inspected by phase contract microscopy, no abnormal morphology was observed.

After 8 days of incubating a printed gel samples without any antibiotics or antimyotics, less than 1 bacterium per 0.9 μL was detected (n = 12).

ECM accumulation

GAG content increased in printed samples over time in incubation to 18.9 ± 4.2 μg/μg DNA (n = 4–17) by 3 weeks (Fig. 6). Printed disks were cultured beyond 3 weeks to ~18 weeks, but GAG level did not change significantly.

Hydroxyproline content increased in the printed samples over time in incubation as well. Hydroxyproline content reached 0.92 ± 0.15 μg/μg DNA (n = 4–17) by 14 weeks (Fig. 7). At 18 weeks, the disks did not appear to change shape grossly when compared to disks exposed to media immediately after printing (Fig. 8).

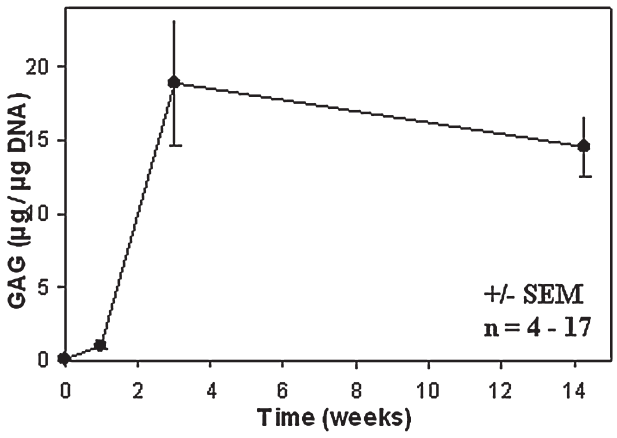


FIG. 6. GAG content DNA normalized with time in culture.

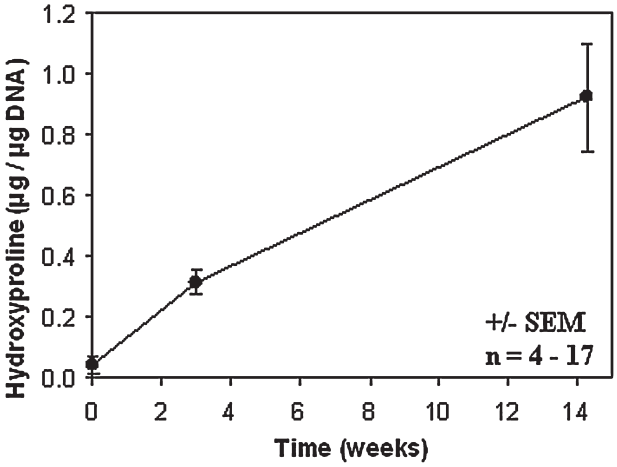


FIG. 7. Hydroxyproline content DNA normalized with time in culture.

Mechanical properties

It was observed that the Young's modulus of samples increased with time after fabrication. The compressive elastic modulus of a typical printed disk that was less than 1 h old was determined to be 1.8 ± 0.1 kPa (n = 6).

Geometric fidelity

When the point maps of the entire printed samples (Fig. 9) were considered, the average height of a single layer was determined to be 0.80 ± 0.03 mm and the RMS surface roughness was 0.33 ± 0.01 mm. When only the points with X-Y coordinates located in the inner region of the printed samples, the edge effect was ignored and the resulting average height was 1.14 ± 0.06 mm and the RMS surface roughness was 0.16 ± 0.02 mm.

When the X-Y error was analyzed at the mid-height plane (Fig. 10), the average X-Y error was found to be 0.58 ± 0.07 mm. The standard deviation of the X-Y error was found to be 0.27 ± 0.03 mm.

DISCUSSION

The objective of this research was to develop a technique for directly fabricating pre-seeded constructs in arbitrary geometries with multi-axial zonal organization. In order for the technique to be considered a feasible tissue-engineering approach, we focused on a set of benchmarks including process viability, process sterility, ECM production by printed samples, and mechanical properties of printed samples.

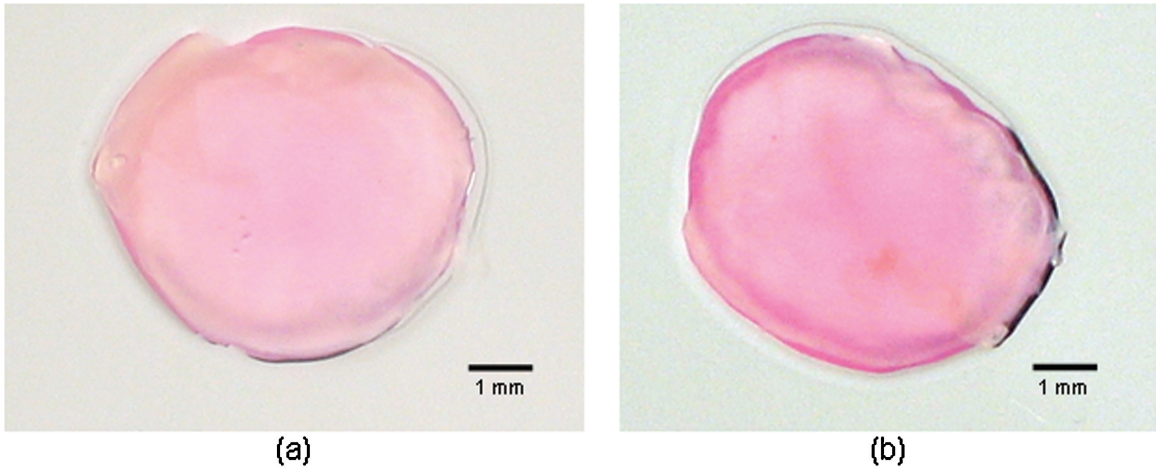


FIG. 8. Printed disks after 1 day (**A**) and 142 (**B**) days in culture. (Color images are available online at www.liebertonline.com/ten).

Samples printed into simple geometries retained their shape for the duration of a 20 week culture. This result points to an advantage of using alginate as a material delivery system for 3-D printing. Other materials proposed for such applications are highly amenable to printing,[22] but do not retain their shape in culture, due to contraction, in the case of collagen, or swelling and dissolution, in the case of pluronic-F127.

The results of the viability test suggest that the printing process, including the cell encapsulation and gel deposition stages, does not have a major harmful impact on the cell viability of printed cells. A 94 ± 5% process viability is adequate for a new tissue-engineering technique. This viability value is markedly higher than other SFF approaches to pre-encapsulated construct fabrication, which are in the range of 60–70%.[20]

The bacteria count of less than 1 bacterium per 0.9 μL of media suggests that the samples were bacteria free and that the sterile envelope technique worked sufficiently well. The autoclave bag served as an inexpensive and disposable sterile envelope that can be fit to a printing workspace of any size. The use of an environmental envelope reduced the demands placed on the sterility of the production site. Furthermore, other than the syringe and syringe tip, the printer itself did not need to be sterilized. This technique would enable future applications in which the maintenance of environmental sterility would otherwise be challenging.

The peak GAG content of 18.9 μg/μg DNA and the peak hydroxyproline content of 0.92 μg/μg DNA were similar to those observed in a number of studies in which bovine articular chondrocytes were seeded onto a variety of substrates (Table 1). This suggests that the printing process did not substaintially interfere with the ability of printed cells to assemble an extracellular matrix.

The elastic modulus of the alginate hydrogel printed samples was higher than the modulus of samples created by some other SFF techniques that created pre-seeded

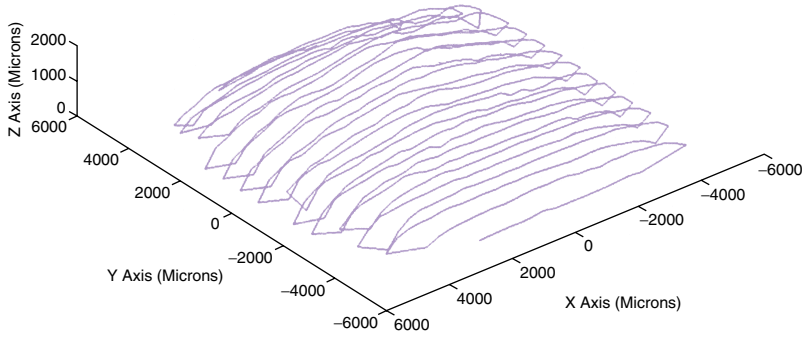


FIG. 9. Centered and truncated CMM data for an 8 × 8 mm printed geometry.

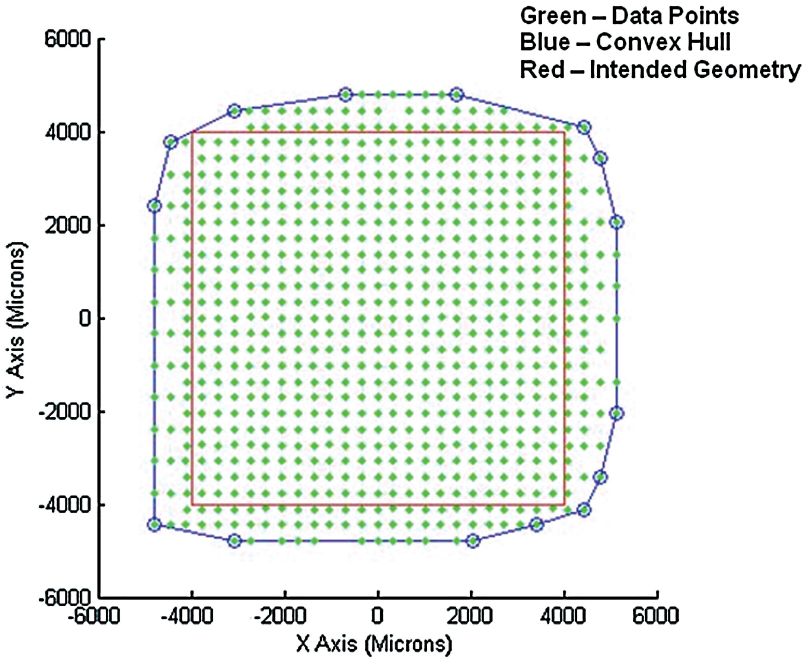


FIG. 10. Cross-section of CMM map truncated at mid-height. (Color images are available online at www.liebertonline.com/ten).

implants. The modulus of alginate-printed samples was higher than those created with the photo-crosslinking SFF technique.[20] Also, alginate hydrogels are much stiffer than those made from pluronic F-127, which has been investigated as a build material for SFF tissue-engineering approaches.[22] Furthermore, the mechanical properties of printed alginate implants could be easily improved through the addition of calcium in or after the printing process.

The tissue-engineering approach detailed herein combines the strengths of molding techniques with those of solid freeform fabrication technology. This technology successfully encapsulates bovine chondrocytes in alginate hydrogel and deposits them in arbitrary geometries while maintaining sterility and viability. Unlike injection molding of pre-seeded alginate hydrogel, this technique does not require molds, nor does it require any custom tooling to fabricate an implant. Also, due to the inherent benefits of SFF, implants with complex geometries can be fabricated that could not otherwise be molded or easily fabricated using other methods such as layering sheets.

This tissue-engineering approach combines the strength and biocompatibility of hydrogel injection molding with the geometric freedom and inherent patient-specificity capabilities of SFF. The method could allow for efficient fabrication of patient-specific implants without the cost and delay normally associated with creating custom tooling. Furthermore, this technique reduces the constraints imposed upon the fabrication environment, which is an important concern for *in situ* and minimally invasive *in vivo* implant fabrication. This technology could enable fabrication of geometrically complex, multiple-material implants that would otherwise not be producible. Also, this approach could enable the fabrication of large implants thatwould otherwise be difficult to seed with cells due to transport limitations.

TABLE 1. COMPARISON OF ECM PROPERTIES

	Alginate beads (weeks)	*Alginate injection molding (weeks)*	*Alginate SFF (weeks)*
GAG (μg/μg DNA)	28[26] (3)	18[28] (10)	18.9 ± 4.2 (3)
Hydroxyproline (μg/μg DNA)	28[26] (3) 1.9[29] (6)	1.8[28] (10)	0.92 ± 0.15 (14)

ACKNOWLEDGMENTS

This work was funded by Cornell University. The authors would also like to thank Suzanne Maher at the Hospital for Special Surgery (New York, NY) for technical assistance with CT scans of ovine meniscus.

REFERENCES

1. Cao, Y., Vacanti, J.P., Paige, K.T., Upton, J., and Vacanti, C.A. Transplantation of chondrocytes utilizing a polymer-cell construct to produce tissue-engineered cartilage in the shape of a human ear. Plast. Reconstr. Surg. **100,** 297, 1997.
2. Kim, W.S., Vacanti, J.P., Cima, L., Mooney, D., Upton, J., Puelacher, W.C., and Vacanti, C.A. Cartilage engineered in predetermined shapes employing cell transplantation on synthetic biodegradable polymers. Plast. Reconstr. Surg. **94,** 233, 1994.
3. Puelacher, W.C., Wisser, J., Vacanti, C.A., Ferraro, N.F., Jaramillo, D., and Vacanti, J.P. Temporomandibular joint disc replacement made by tissue-engineered growth of cartilage. J. Oral Maxillofac. Surg. **52,** 1172, 1994.
4. Weng, Y., Cao, Y., Silva, C.A., Vacanti, M.P., and Vacanti, C.A. Tissue-engineered composites of bone and cartilage for mandible condylar reconstruction. J. Oral Maxillofac. Surg. 59, 185, 2001.
5. Ibarra, C., Jannetta, C., Vacanti, C.A., Cao, Y., Kim, T.H., Upton, J., and Vacanti, J.P. Tissue engineered meniscus: a potential new alternative to allogeneic meniscus transplantation. Transplant. Proc. **29,** 986, 1997.
6. Kojima, K., Bonassar, L.J., Ignotz, R.A., Syed, K., Cortiella, J., and Vacanti, C.A. Comparison of tracheal and nasal chondrocytes for tissue engineering of trachea. Ann. Thorac. **76,** 1884, 2003.
7. Mizuno, H., Roy, A.K., Vacanti, C.A., Kojima, K., Ueda, M., and Bonassar, L.J. Tissue-engineered composites of annulus fibrosus and nucleus pulposus for intervertebral disc replacement. Spine **29,** 1290, 2004.
8. Kamil, S.H., Kojima, K., Vacanti, M.P., Bonassar, L.J., Vacanti, C.A., and Eavey, R.D. In vitro tissue engineering to generate a human-sized auricle and nasal tip. Laryngoscope **113,** 90, 2003.
9. Puelacher, W.C., Mooney, D., Langer, R., Upton, J., Vacanti, J.P., and Vacanti, C.A. Design of nasoseptal cartilage replacements synthesized from biodegradable polymers and chondrocytes. Biomaterials **15,** 774, 1994.
10. Puelacher, W.C., Vacanti, J.P., Ferraro, N.F., Schloo, B., and Vacanti, C.A. Femoral shaft reconstruction using tissue-engineered growth of bone. Int. J. Oral Maxillofac. Surg. **25,** 223, 1996.
11. Vacanti, C.A., Bonassar, L.J., Vacanti, M.P., and Shufflebarger, J. Replacement of an avulsed phalanx with tissue-engineered bone. N. Engl. J. Med. **244,** 1511, 2001.
12. Hung, C.T., Lima, E.G., Mauck, R.L., Taki, E., LeRoux, M.A., Lu, H.H., Stark, R.G., Guo, X.E., and Ateshian, G.A. Anatomically shaped osteochondral constructs for articular cartilage repair. J. Biomech. **36,** 1853, 2003.
13. Cao, Y., Rodriguez, A., Vacanti, M., Ibarra, C., Arevalo, C., and Vacanti, C.A. Comparative study of the use of poly(glycolic acid), calcium alginate and pluronics in the engineering of autologous porcine cartilage. J. Biomater .Sci. **9,** 475, 1998.
14. Chang, S.C., Rowley, J.A., Tobias, G., Genes, N.G., Roy, A.K., Mooney, D.J., Vacanti, C.A., and Bonassar, L.J. Injection molding of chondrocyte/alginate constructs in the shape of facial implants. J. Biomed. Mat. Res. **55,** 503, 2001.
15. Klein, T.J., Schumacher, B.L., Schmidt, T.A., Li, K.W., Voegtline, M.S., Masuda, K., Thonar, E.J., and Sah, R.L. Tissue engineering of stratified articular cartilage from chondrocyte subpopulations. Osteoarth. Cart. **11,** 595, 2003.
16. Kim, T.K., Sharma, B., Williams, C.G., Ruffner, M.A., Malik, A., McFarland, E.G., and Elisseeff, J.H. Experimental model for cartilage tissue engineering to regenerate the zonal organization of articular cartilage. Osteoarth. Cart. **11,** 653, 2003.
17. Ng, K.W., Wang, C.C., Mauck, R.L., Kelly, T.A., Chahine, N.O., Costa, K.D., Ateshian, G.A., and Hung, C.T. A layered agarose approach to fabricate depth-dependent inhomogeneity in chondrocyte-seeded constructs. J. Orthop. Res. **23,** 134, 2005.
18. Sun, W., Starly, B., Darling, A., and Gomez, C. Computer-aided tissue engineering: application to biomimetic modeling and design of tissue scaffolds. Biotechnol. Appl. Biochem. **39,** 49, 2004.
19. Ballyns, J., Gleghorn, J., Niebrzydowski, V., Rawlinson, J., Maher, S., and Bonassar, L.J. Tissue engineering of meniscus using microCT imaging, CAD and injection molding. Abstract presented at the 51st Annual Meeting of the Orthopaedic Research Society, Washington D.C., 2005. Abstract no. 292.
20. Busaina, D., Hunt, E., and Boland, T. Rapid prototyping of tissue-engineering constructs, using photopolymerizable hydrogels and stereolithography. Tissue Eng. **10,** 1316, 2004.
21. Khalil, S., Nam, J., and Sun, W. Multi-nozzle deposition for construction of 3D biopolymer tissue scaffolds. Rapid Prototyp. J. **11,** 9, 2005.
22. Smith, C.M., Stone, A.L., Parkhill, R.L., Stewart, R.L., Simpkins, M.W., Kachurin, A.M., Warren, W.L., and Williams, S.K. Three-dimensional BioAssembly tool for generating viable tissue-engineered constructs. Tissue Eng. **10,** 1566, 2004.
23. Malone E., Rasa K., Cohen D. L., Isaacson T., Lashley H., and Lipson H. Freeform fabrication of 3D zinc-air batteries and functional electro-mechanical assemblies. Rapid Prototyp. J. **10,** 58, 2004.
24. Genes, N.G., Rowley, J.A., Mooney, D.J., and Bonassar, L.J. Effect of substrate mechanics on chondrocyte adhesion to modified alginate surfaces. Arch. Biochem. Biophys. **422,** 161, 2004.
25. Kim, Y.J., Sah, R.L., Doong, J.Y., and Grodzinsky A.J. Fluorometric assay of DNA in cartilage explants using Hoechst 33258. Anal. Biochem. **174,** 168, 1988.
26. Enobakhare, B.O., Bader D.L., and Lee D.A. Quantification of sulfated glycosaminoglycans in chondrocyte/alginate cultures, by use of 1,9-dimethylmethylene blue. Anal. Biochem. **243,** 189, 1996.
27. Neuman, R.E., and Logan, M.A. The determination of hydroxyproline. J. Biol. Chem. **184,** 299, 1950.
28. Kim, Y.J., Bonassar, L.J., and Grodzinsky, A.J. The role of cartilage streaming potential, fluid flow and pressure in the stimulation of chondrocyte biosynthesis during dynamic compression. J. Biomech. **28,** 1055, 1995.
29. Beekman, B., Verzijl, N., Bank, R.A., von der Mark, K., and TeKoppelle, J.M. Synthesis of collagen by bovine

chondrocytes cultured in alginate; posttranslational modifications and cell-matrix interaction. Exp. Cell Res. **237,** 135, 1997.

30. Hott, M.E., Megerian, C.A., Beane, R., and Bonassar, L.J. Fabrication of tissue engineered tympanic membrane patches using computer-aided design and injection molding. Laryngoscope **114,** 1290, 2004.
31. Ragan, P.M., Chin, V.I., Hung, H.H., Masuda, K., Thonar, E.J., Arner, E.C., Grodzinsky, A.J., and Sandy, J.D. Chondrocyte extracellular matrix synthesis and turnover are influenced by static compression in a new alginate disk culture system. Arch. Biochem. Biophys. **383,** 256, 2000.

Address reprint requests to:
Lawrence J. Bonassar, Ph.D.
Department of Biomedical Engineering
Cornell University
218 Upson Hall
Ithaca, NY 14853

E-mail: lb244@cornell.edu